



A validated numerical investigation of the ceiling fan's role in the upper-room UVGI efficacy

George Pichurov ^a, Jelena Srebric ^{b,*}, Shengwei Zhu ^c, Richard L. Vincent ^d, Philip W. Brickner ^d, Stephen N. Rudnick ^e

^a Technical University of Sofia, Department of Hydroaerodynamics and Hydraulic Machines, Sv. Kliment Ohridski 8, Sofia 1000, Bulgaria

^b University of Maryland, Department of Mechanical Engineering, 3143 Glenn L. Martin Hall, College Park, MD 20742, United States

^c Huazhong University of Science and Technology, School of Architecture and Urban Planning, 1037 Luoyu Road, Hongshan District, Wuhan 430074, PR China

^d The Icahn School of Medicine at Mount Sinai, Department of Medicine, Division of General Internal Medicine, One Gustave L. Levy Place, Box 1087, New York, NY 10029, United States

^e Harvard School of Public Health, Department of Environmental Health, 665 Huntington Ave, Rm 1-B21, Boston, MA 02115-6021, United States



ARTICLE INFO

Article history:

Received 26 September 2014

Received in revised form

9 December 2014

Accepted 26 December 2014

Available online 9 January 2015

Keywords:

Upper-rooms germicide irradiation (UVGI)
Microorganism susceptibility to ultraviolet (UV) radiation

Eulerian and Lagrangian CFD

Particle simulations

Ceiling fan

ABSTRACT

This investigation quantifies the upper-room ultraviolet germicidal irradiation (UVGI) efficacy in a room with a ceiling-mounted fan that blew air either upwards or downwards at three rotational speeds. The numerical modeling deployed a steady-state passive scalar (Eulerian) and particle tracking (Lagrangian) CFD with a rotating reference frame. Two wall-mounted fixtures horizontally collimated the irradiance field, which was measured with a flat sensor and imported into the numerical models. This study predicted the UVGI efficacy under an extreme range of microorganism susceptibilities to define relationships between the system performance and operational parameters. A mathematical expression with general validity for fraction remaining under perfect air-mixing conditions was analytically developed and used as a performance benchmark. The CFD predictions were validated by the experimental data, expressed as a fraction remaining at the room exhaust for two different microorganisms. Numerical predictions were in a good agreement with the experimental data. In general, the Lagrangian predictions agreed better with the measured data than the Eulerian predictions. Inclusion of a rotating fan significantly improved UVGI performance, but there was no benefit from increasing the fan speed beyond certain values. For this investigation where the microorganism source is located below the fan, the UVGI system performed most efficiently when the fan blew upward, with the optimal performance achieved for the moderate rotational speed of 107 rpm. The highest upper-room UVGI efficacy for this fan setup is due to the airflow and UV light fields enabling a delivery of the highest amount of UV irradiation to the microorganism.

© 2015 Elsevier Ltd. All rights reserved.

1. Introduction

Ultraviolet germicidal irradiation (UVGI) has gained popularity as a method to reduce the risk of transmitting airborne pathogens in hospital rooms. Ultraviolet (UV) radiation, UV-C bandwidth of 100–280 nm has the potential to damage the DNA of microorganisms, leading to their potential inactivation [1]. The probability of inactivation depends on the UV dose received by the microorganism, and on the microorganism's vulnerability to UV radiation, which is quantified by a susceptibility constant. The susceptibility

of a given microorganism is partially a property of its DNA and of the environmental humidity, and can be measured under controlled conditions. The most practical way to increase the probability of inactivation is to increase the ultraviolet dose received by the microorganism. This is a challenging task because the UV radiation bandwidth that damages the microorganism's DNA is also harmful to human occupants and is responsible for side effects like erythema (redness of the skin) and photokeratitis ("welder's flash" or "snow-blindness") [2]. In order to protect occupants from exposure to UV radiation, the radiation source is installed in specially designed louvered fixtures that horizontally collimate the UV radiation in the upper part of the room, giving the technology its name (upper-room UVGI). Although there are self-

* Corresponding author. Tel.: +1 301 405 7276; fax: +1 301 405 2025.

E-mail address: j.srebric@umd.edu (J. Srebric).

contained UV air cleaning devices, comprised of an air-suction enclosed box with UV source, the upper-room UVGI is the most widely applied technology for disinfecting large volumes of air in high-risk congregate settings [3–5].

Numerical predictions by Zhu et al. [6–8], demonstrated that upper-room UVGI efficiency is improved by a rotating ceiling fan. The fan enhances the air movement and facilitates the transport of the microorganisms into the irradiated upper-room. Along with the fan rotational speed and blow direction (upwards or downwards), its physical size and the number and shape of fan blades were identified as important operational parameters for correct simulation of the room airflow. Zhu et al. solved a passive scalar equation for the viable microorganism mass fraction, which lies in the origin of the Eulerian method. Gilkenson and Noakes [9] pointed out that validation is necessary before passive scalar models can be reliably used for quantitative predictions, which additionally motivated the validations in the present study.

Several studies employed the passive scalar model to calculate the ultraviolet dose distribution in a room using a generic transport equation where the fluence rate appears as a source term [10,11]. This approach calculated the dose received by inlet air, which is not identical to the dose received by microorganisms. To resolve this issue, Sung and Kato [12] calculated a transport equation for the dose received by air supplied from contaminant source using the concept of scales of ventilation efficiency [13,14]. Applying this dose in the decay ratio (equation (1)) produced different values for the viable mass fraction other than calculating it directly, such as in Ref. [6] and equation (2). The explanation is that the average dose may not be applied over the average concentration because inactivation is based on an exponential relationship, and the average of exponents is not identical to an exponent from an average. Therefore, if UV dose shall be used for prediction of microorganism inactivation and fraction remaining, it must be calculated by the Lagrangian method.

The Lagrangian method predicts the trajectories and UV doses accumulated by individual microorganisms. The survival probability of each microorganism and the fraction of viable microorganisms at the room exhaust are then evaluated. A Lagrangian particle transport model has been successfully utilized by Refs. [15] and [16] to estimate UVGI efficacy in ventilated premises without a fan. The studies concluded that UVGI efficacy decreases with an increase in air exchange rate, due to reduced microorganism residence time inside the irradiation zone. Ghia et al. [17] employed the Lagrangian Discrete Phase Model (DPM) for their study of aerosol dispersion under different ventilation conditions. In their study, they allowed the particles to agglomerate and bounce off walls. The evaporation of droplets was not considered, and it was not included in the present study because microorganisms were nebulized and the liquid evaporated almost immediately. In previous research, particle settling and wall absorption have been found to be negligible by Heidarnejad and Srebric [18], so these transport phenomena were not included.

Based on the literature review, no studies thus far have employed and directly compared both the Lagrangian and Eulerian predictions in ventilated rooms with a rotating fan. For each set of conditions in the present study, the fraction of remaining microorganisms at exhaust was predicted using both methods over a wide range of microorganism susceptibilities. An analytical expression for the fraction remaining in case of perfect mixing was developed and used for comparison with the simulated cases. Predictions were compared to experimental measurements for two microorganisms with about a four-fold difference in UV susceptibility [19]. It is important to notice that the Computational Fluid Dynamics (CFD) predictions presented here had been conducted before these experimental results became available.

2. Methodology

The present paper uses the first-order decay model in which the probability (P) of a microorganism to survive ultraviolet germicidal irradiation decreases exponentially with the quantity of the ultraviolet dose received (D , $[J/m^2]$), and the microorganisms' susceptibility to radiation (z , $[m^2/J]$) [12,20]:

$$P = e^{-zD} \quad (1)$$

The dose D is the time integral of the UV fluence rate E [W/m^2] to which a microorganism is exposed. The probability P is also equal to the fraction of surviving microorganisms that has been exposed to a dose D , [10]. The Lagrangian method directly evaluates the survival probability P of each microorganism from the dose it receives, while the Eulerian uses the rate of inactivation as a sink term in the species conservation equation (2). The work of [20] acknowledges that not all microorganisms follow the first-order model of equation (1), which may partly explain the measurement uncertainty of microorganism susceptibility. It should be noted that both the Eulerian and Lagrangian methods were applied based on the known flow field from the CFD simulations. In addition, the methods only considered the influence of flow field on passive scalar or particles, and ignored their reactions on flow field.

2.1. Eulerian method

The Eulerian method has been widely applied to performance predictions of upper room UVGI systems in a steady indoor environment in previous studies [6,18]. The method is based on the notion that microorganisms occupy a certain fraction of the air volume. The fraction of viable microorganisms, C , is described by a passive scalar equation:

$$\frac{\partial}{\partial x_j} (C u_j) - \frac{\partial}{\partial x_j} \left((\lambda + \lambda_t) \frac{\partial C}{\partial x_j} \right) = -z E C \quad (2)$$

E is the fluence rate [W/m^2], x_j are spatial coordinates [m], u_j are velocity components [m/s], λ and λ_t are laminar and turbulent diffusivity [m^2/s], and summation is applied over repeating indices. z is the UV susceptibility constant of the microorganism of interest [m^2/J]. The sink term on the right-hand side is the rate of microorganism inactivation based on first order kinetics. To model this term in the employed CFD package, i.e. Ansys Fluent 13.0 [21], we wrote a user-defined function. After the viable microorganism mass fraction is converged, its value at exhaust C_{UVon} [kg/kg] is divided by the microorganism mass fraction with deactivated UV irradiation C_{UVoff} [kg/kg] to obtain a ratio popularly known as fraction remaining, f_{rm} :

$$f_{rm} = \left. \frac{C_{UVon}}{C_{UVoff}} \right|_{exhaust} \quad (3)$$

It is important that the microorganism generation rate is identical in both the UV and non-UV regime of the UVGI system, so that the decrease of the exhaust mass fraction can be solely attributed to the UV field. Microorganisms are introduced in the domain via a velocity inlet, but because of scalar gradients in the vicinity of the injector, the microorganisms also penetrate the domain via scalar diffusion. The scalar gradients will change when the UV field is turned on and the diffusive flux of microorganisms will also change. No reliable method existed to quantify this scalar diffusive flux, so the best approach to guarantee a fixed generation rate was to disable inlet diffusion for scalar variables. This technique is also popularly used to accurately simulate local mean age-of-air elsewhere.

The fraction remaining calculated by equation (3) measures the integral ability of the upper-room UVGI system to inactivate airborne microorganisms, and is used as a quantitative factor for comparing system efficacy under different setups.

2.2. Lagrangian method

The Lagrangian method represents the microorganisms as discrete particles and predicts their trajectories with the use of a discrete phase model (DPM). The UV dose accumulated by each particle is calculated according to the expression [16]:

$$D = \int E dt \approx \sum_i E_i \Delta t_i \quad (4)$$

where Δt_i is a particle tracking time step [s] and E_i is the local (cell) fluence rate [W/m^2] to which the particle is exposed. A user-defined function was written to calculate this dose in the CFD package. The time step Δt_i is evaluated from the particle path step, whose length can be either a constant or a fraction of the local cell size. Sensitivity analysis with different settings, including a constant length of 0.5 mm and 5 steps per mesh cell, did not indicate impact on the results.

When integrating the particle tracks, the type of velocity formulation inside the fan rotational zone becomes important. The relative velocity formulation predicts unrealistic spiraling particle tracks inside the rotating reference frame, but allows for quicker particle data integration than the absolute velocity formulation. Nevertheless, both formulations predict identical residence times of the particles, and therefore accumulated UV dose, because the increased track length in the relative velocity formulation is compensated by the increased particle velocity due to the added relative velocity component. As a result, the absolute velocity formulation was used to visualize the particle trajectories, but the relative velocity formulation was used for dose value integration.

A second user-defined function was written to generate a file with the dose values accumulated for all particles that left the room through the exhaust. The survival probability of each microorganism was then calculated according to equation (1) after being assigned a z-value. To determine whether the microorganism survived or not, a random number in the range [0, 1] was individually generated for each microorganism, and then compared to its survival probability. If the random number exceeded the probability, the microorganism was considered inactivated. The number of surviving microorganisms n was divided by the total number of microorganisms N at exhaust to yield the fraction remaining f_{rm} :

$$f_{rm} = \frac{n}{N}_{\text{exhaust}} \quad (5)$$

Even though a stochastic procedure was used to determine the surviving chances of each microorganism, numerous applications of the procedure produced consistent results with variability of no more than 1–2 percent, mainly because of the large sample of particles involved (more than 1200).

The fraction of remaining microorganisms calculated by both the Eulerian (equation (3)) and Lagrangian (equation (5)) methods were used to directly compare their numerical predictions and to determine their agreement with physical measurements for the studied configurations. The results were also compared to the analytically developed regime of perfect mixing.

2.3. Fraction remaining for the perfect mixing flow regime

By definition, perfect mixing is a flow with infinite diffusivity [22]. An infinite diffusion coefficient forces the gradient term in the

species transport equation to become zero. This results in uniform distribution of the species throughout the whole room, including the room exhaust. The analytical derivation of fraction remaining in a case of perfect mixing starts with the balance equation for the viable microorganism mass fraction. Under steady-state conditions, the rate of microorganism generation is equal to the rate of removal through exhaust and the rate of microorganism inactivation by the UV field. The rate of inactivation equals the sink term of equation (2) integrated over the whole domain:

$$\int CzEdm = Cz \int Edm = Cz\bar{E}M \quad (6)$$

The viable mass fraction C [kg/kg] can be removed from the integral since it is uniform in a perfectly mixed flow. \bar{E} [W/m^2] is the average fluence rate in the room, M [kg] is the mass of air in the room. Viable microorganisms are removed through the exhaust at a rate equal to the product of viable microorganism mass fraction and air mass flow rate, $C\dot{m}$. Under steady-state conditions the sum of these two terms equals the microorganism generation rate (G [kg/s]):

$$G = Cz\bar{E}M + C\dot{m} \quad (7)$$

After rearranging, the viable microorganism mass fraction in the room (and hence the exhaust) is:

$$C = \frac{G/\dot{m}}{1 + z\bar{E}M/\dot{m}} \quad (8)$$

The ratio of air mass over mass flow rate M/\dot{m} in the denominator is known as the nominal time constant (τ_n) [22], which is the inverse of air exchange rate n [s^{-1}]. In the absence of UV radiation, the average fluence rate is zero and the microorganism mass fraction is G/\dot{m} . Dividing equation (8) by this ratio is by definition (see eq. (3)) the fraction remaining in case of perfect mixing:

$$f_{rm} = \frac{1}{1 + z\bar{E}\tau_n} \quad (9)$$

Predictably, the expression asymptotically reaches zero when either z or E approaches infinity. Since all microorganisms are transported to the upper room in case of perfect air mixing, they will receive a lethal dose of radiation if their susceptibility or the fluence rate is infinitely high. It is also observed that increasing the air exchange rate, hence reducing the nominal time constant τ_n , negatively affects the UVGI system's performance.

Perfect air mixing may not necessarily offer the best UVGI system performance. For example, if the contaminant source is generated inside the upper-room region or near the room exhaust, mixing should be avoided. However, in hospital rooms the airborne pathogens are generated in the lower-room and increased mixing would generally be beneficial.

The perfect mixing expression for fraction remaining given by equation (9) is a special case of the general sigmoid function, which can be used to fit the fraction remaining for any real-room setup:

$$f_{rm} = a + \frac{1}{b + cz} \quad (10)$$

where, a , b and c are function coefficients, and z is the susceptibility constant.

3. Experimental validation methods

This study examines the upper-room UVGI efficacy in an experimental chamber located at the Harvard School of Public

Health, described, along with the experimental methods, in Rudnick et al. [19]. The room had dimensions of $4.6 \times 2.97 \times 3.05$ m, and is shown with the computational mesh in Fig. 1. Fresh air was supplied near the ceiling and exhausted oppositely, near the floor. The air supply grille is split into two partitions, one of them supplying 45% of the flow at an angle 30° to the surface normal vector. The airflow rate used in the experiments and computations is 6 ACH, which translates to a normal velocity of 0.6 m/s over the inlet surface area. The nominal time constant required by the perfect-mixing calculations is the inverse of the air exchange, $\tau_n = 600$ s.

An axial 5-blade ceiling fan (Maker: Hunter; Model: 28415) was installed in the middle of the ceiling with the mid-plane of the blades 35 cm below the ceiling. The purpose of the fan is to increase the microorganisms' visitation rate in the upper room, not to provide cooling or ventilation. The fan measures 132 cm in diameter with blades that are 52 cm long, 0.6 cm thick and have width of 14 cm at the base and 16 cm at the tip as shown in Fig. 2. The pitch angle of the blades is 11.5° and the deflection of their tips due to gravity is 2.5 cm relative to the base.

Measurement data were collected for two microorganisms: *Bacillus atrophaeus*, with UV susceptibility of 0.018 ± 0.0017 m²/J, and *Mycobacterium parafortuitum*, with UV susceptibility of 0.074 ± 0.011 m²/J [19]. Microorganisms were nebulized into the room through a spherical injector of 75 mm diameter, located in the center of the room 1.5 m above the floor with a supply rate of 12 L/min. Two UVGI wall fixtures, each containing one 25 W tubular lamp, were installed on the opposite short walls of the room. They were mounted 2.26 m high with the lamp front extending 15 cm away from the back wall and 60 cm away from the adjacent walls. The fluence rates for the upper room were measured in 6 horizontal planes at 35 locations per plane for a total of 210 data points. These locations are listed in Ref. [23] and data published in Ref. [19].

4. CFD simulation parameters

Several versions of the computational mesh were generated to test the grid independence. For a mesh with 1 million cells, the maximum cell skewness was 167° , and with mesh size of 1.7 million, the maximum cell skewness decreased to 157° . The mesh density did not have an effect on the results for the control simulation case, but nevertheless the higher mesh density was used in subsequent computations (Fig. 1). The fan is modeled by a rotating reference frame with a radius of 112 cm. It is desirable that this

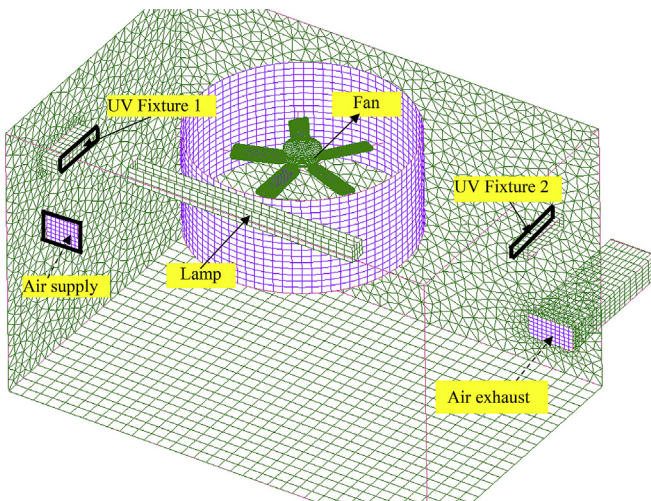


Fig. 1. Experimental room geometry and computational mesh.

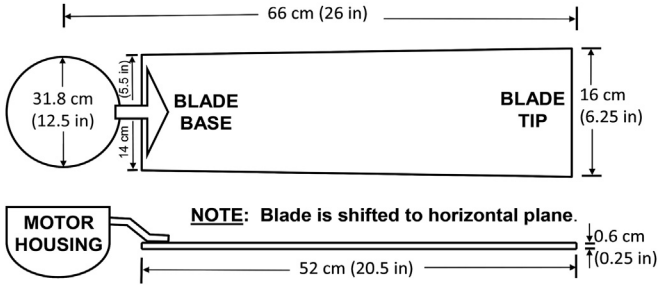


Fig. 2. Fan and blade geometry.

radius is as large as possible, but without intersecting any non-rotational surfaces. The blades' surface is set to rotate at the rotation rate of the rotating reference frame and the hub (or housing) surface of the fan is fixed in relation to the absolute reference frame to properly reflect the real fan operation. Special attention was paid to the geometry and meshing of the fan, with the highest emphasis on the blades, including the rounding at the tips, as shown on Fig. 3(a), and deflection due to weight. They are meshed with a mixture of structured and unstructured patterns to enable better alignment of the grid with the flow direction. A boundary layer mesh of four cell layers was extruded outward from the blade surface and is shown on Fig. 3(b) for a single blade.

Measurement data for the fluence rate was imported into the CFD package as a scalar variable, intended to be used by both the Lagrangian and Eulerian methods. The fluence rate data for this particular lamp fixture and experimental setup are available in the literature [19]. The fluence rate data were interpolated using the software built-in interpolation methods, but without much effect from the interpolation. Fluent import methods consistently produced, even with disabled interpolation, a uniform, non-zero fluence rate in the entire domain, even outside of the irradiated zone. To repair this, we wrote a user-defined function to restrict the fluence rate only within the irradiated zone ($Z = 2.13\text{--}2.85$ m) after import. The effect of fluence rate modeling representation on the predictions of UVGI efficiency was studied by Heidarinejad and Srebric [18], who found that a manual, multi-volume segregation of the fluence rate was sufficiently accurate. The direct import, used here, offers better detail and saves the effort for manually partitioning the irradiated zone. A detailed representation of the fluence rate becomes progressively less important with increased air mixing and for a perfectly mixed flow because it is identical to a uniform bulk average representation. For this particular room and UV lamp configuration, the room-average fluence rate \bar{E} was calculated as 67 mW/m^2 . This value is used by the perfect mixing model (equation (9)), and it has to be the average for the whole computational domain and not only for the upper room zone, which is commonly used elsewhere.

Table 1 summarizes the boundary conditions used in the simulated setups. The exhaust diffuser has been modeled as a pressure outlet that extended downstream the room exhaust to avoid reverse flow. The standard $k-\epsilon$ model was employed for the non-rotating fan case because it was assumed that it could adequately represent the supply jet momentum that governs the room air distribution. When the fan was operated, however, its induced momentum was crucial for the airflow and turbulence predictions, and thus a low-Reynolds number variation of the realizable $k-\epsilon$ model was utilized. The software package [21] states that this model offers certain advantages over the standard and possibly over the RNG $k-\epsilon$ models because it has a physically correct representation of certain model terms that the other models lack. However, it was later discovered that the model contains an

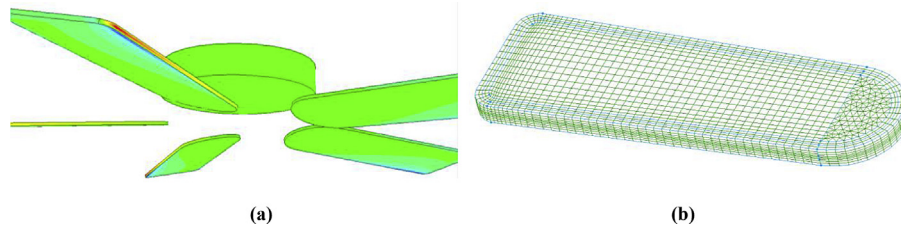


Fig. 3. (a) CFD model of the fan and (b) boundary layer mesh around a fan blade.

undesirable strain term which only appears in problems that contain an absolute and a rotating reference frame, and in this case the generation of turbulent viscosity can be over-predicted. This may explain the report of excessive turbulent viscosity ratio in certain cells during the iterations, and why the degree of mixing was generally over-predicted in some of the simulated cases. The Reynolds stress model was also attempted to accurately resolve the downward blow of the fan; however, the convergence difficulties outweighed its advantages. The Boussinesq approximation was used to model the upward momentum created by heat sources, namely the UV fixtures and the visible light lamp. The PRESTO algorithm for pressure–velocity coupling was used, the spatial discretization of the momentum, k and ϵ equations were second-order upwind, and for the energy and passive scalar equations were first-order upwind. Because of the large number of computational cells and the possible presence of dynamic effects due to fan rotation, the convergence was satisfied with the criterion of $1 \cdot 10^{-3}$, in some cases with the criterion of $5 \cdot 10^{-4}$. The laminar and turbulent Schmidt numbers were 1.0. The scalars converged to a criterion of 10^{-12} , but as mentioned before, the scalar diffusion at the microorganism source had to be disabled, which created nonphysical (below 0 and beyond 1) concentrations in certain cells adjacent to the microorganism injector. However, the concentration field in the room and its value at the exhaust converged accurately to the mentioned criteria, so the Eulerian predictions were uncompromised. The calculations were performed in parallel on 4 computational nodes using Ansys Fluent 13.0 package [21], with convergence time ranging between 6 and 24 h per case.

The Lagrangian simulation used massless particles, because microorganisms were nebulized with a very small momentum and immediately vaporized into microscopic particles that would passively follow the airflow, especially when created by mechanical ventilation. The turbulence effects on the particles have been accounted for by the discrete random walk model [21]. This avoids the effect that all particles follow identical trajectories when injected from a small source. Moreover, the simulations supposed

that the particles would rebound to the air after their collision with any solid surface. This assumption might underestimate the UV dose as the particles could receive more UV irradiation when they were attached to the surfaces within the UV irradiation zone. However, the assumption was necessary because the existing literature does not provide the probability for particles to settle down onto the surfaces made from plastics, as well as how long the particles would stick onto the surfaces. In addition, the assumption was reasonable, as the underestimation should be very small, because the particles would generally rebound to the air due to the difficulty to settle down onto the plastic surfaces and then stay there for a relatively long time in a flow field with rapid air movement.

Seven cases were simulated that comprised of 3 fan speeds (low, medium, high) and 2 fan directions (upward and downward), plus one control case with non-rotating fan, which are listed in Table 2.

For simulation of microorganism inactivation, the present study employed twenty different values of susceptibility including: $1 \cdot 10^{-4}$, $4 \cdot 10^{-4}$, $1.4 \cdot 10^{-3}$, $4 \cdot 10^{-3}$, 0.01, 0.018, 0.03, 0.045, 0.07, 0.12, 0.18, 0.28, 0.4, 0.6, 1, 1.5, 3, 6, 20 and $100 \text{ m}^2/\text{J}$. This range is wide enough to cover all existing microorganisms and derive a functional relationship between susceptibility and fraction remaining, which is important for the analysis of system behavior. These z-values do not necessarily correspond to actual microorganisms, but were selected to create smooth curves and minimize the interpolation error when evaluating the fraction remaining for an arbitrary pathogen. Such an approach is justified by the fact that measured values of microorganism susceptibility vary between studies and also with relative humidity (McDevitt et al. [24]) and because experimental data for susceptibility in this study became available after the simulations. In addition, once its computational procedure is completed, the Lagrangian method would allow direct evaluation of fraction remaining for arbitrary z-value at no extra cost.

5. Results

For each case, the isothermal and non-isothermal flow fields were converged. The heat sources had negligible effects on the flow compared to the fan and air supply momentum for the studied cases, so simulations could safely be treated as isothermal. The twenty species distributions were calculated according to equation (2), and their fraction remaining was determined by equation (3). The particle trajectories were predicted, and the accumulated UV doses were calculated. The twenty z-values were introduced, and

Table 1
Simulation boundary conditions.

Inlet	Velocity 0.6 m/s normal, 0.34 m/s tangential in 45% of the area (6 ACH). Turbulence intensity 20%, hydraulic diameter 0.3 m. Temperature 21 °C.
UV fixtures	Heat output 20 W (two LIND 24-EVO wall fixtures with 25 W power supply each).
Visible light lamp	Heat output 57 W.
Exhaust	Static pressure = 0, all other quantities zero normal gradient.
Microorganisms supply	12 L/min (equivalent to 0.0113 m/s over the inlet area). Temperature 21 °C. In Eulerian method, microorganism mass fraction C = 1. In Lagrangian method, particles were assumed to be mass-less.
Walls	No-slip conditions at each solid surface. Fan blade surfaces rotate with the rotation speed of the rotating reference frame.

Table 2
Simulated cases.

Blow direction	None	Upward			Downward		
		Low	Medium	High	Low	Medium	High
Fan speed	N/A 0 rpm	61 rpm	107 rpm	176 rpm	61 rpm	107 rpm	176 rpm
Case label	1	2	3	4	5	6	7

the stochastic inactivation algorithm of the Lagrangian method was deployed to determine the number of surviving microorganisms at exhaust and the fraction remaining according to equation (5). For each simulated case, Eulerian and Lagrangian predictions of fraction remaining are compared over the full susceptibility range to the perfect mixing regime and to the experimental data for the two pathogens [19] with their mean and 95% confidence intervals.

5.1. Case 1 (non-rotating fan)

The room airflow in this simulation setup is entirely governed by the air supply momentum. Fig. 4 shows a flow undisturbed by internal blockages, such as furniture and people. The jet from the grille diffuser impinges on the opposite wall to form lower and upper circulation zones with the lower one being more distinguished. Since uniform vector lengths are used in the figure, the circulation zones are actually weaker than they appear and could be easily disturbed by a blowing fan.

Lagrangian predictions of particle trajectories used the random walk model [21]. The effect of the random turbulent fluctuations on the particles was accounted for and their trajectories diversified. Otherwise, particles would follow identical trajectories because they are injected from a point source at a very low velocity. Fig. 5 shows a single particle track colored by its accumulated dose. The particle dose that indicated by color, only changes in the irradiated upper room, but remains unchanged in the rest of the space. This specific particle makes several runs through the irradiated zone before leaving the room through the exhaust. All simulated particles managed to leave the room as long as the particle tracking integration time was long enough.

Fig. 6 shows a logarithmic plot of the fraction remaining f_{rm} vs. susceptibility z , calculated by both the Eulerian and Lagrangian methods. The agreement is relatively satisfactory, with both methods predicting an asymptotic value for the fraction remaining of approximately 0.20 when susceptibility approaches infinity. The fraction remaining in the case of perfect mixing according to equation (9) is plotted for comparison. It is apparent that the system's performance is inferior to the perfect mixing one. According to the simulation results by the Eulerian method, as shown in Fig. 7, any microorganism that enters the upper room is effectively

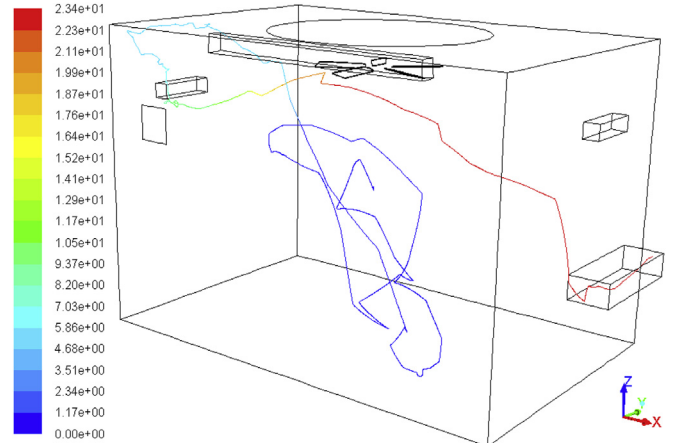


Fig. 5. A single particle track colored by dose D [J/m^2].

inactivated, however due to the limited air mixing, not all microorganisms are actually transported to the irradiated zone. Air mixing is an important transport factor, and can be strongly augmented by a rotating fan, which is illustrated by the results in the forthcoming sections.

5.2. Case 2 (low-speed upward blowing fan)

The rotating fan enhances the microorganisms' mobility and their visitation rate in the irradiated zone increases. Particle tracks also become notably longer. Therefore, the exposure of microorganisms to UV irradiation is significantly longer, and the accumulated dose is significantly larger when the fan is operating. Fig. 8 shows predictions of the fraction remaining versus microorganism susceptibility. The Lagrangian predictions are in excellent agreement with the Eulerian, and are also independent of the particle time step. A notable difference with the non-rotating fan case is that the fraction remaining approaches zero when z -value approaches infinity. This observation was common for all upward blowing fan cases, which displayed performance identical to the perfect mixing case; thus they are all compared to it later, in Fig. 18. Fig. 8 also presents the mean and 95% confidence interval of

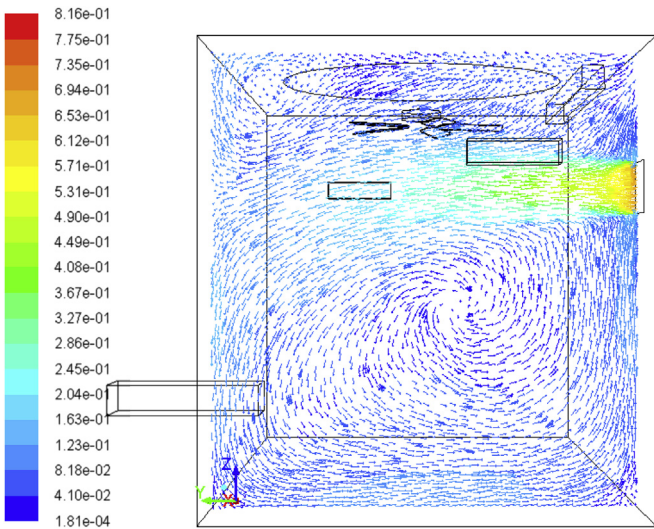


Fig. 4. Velocity vectors in a vertical plane through the air supply diffuser (non-rotating fan) [m/s] (note: vectors are colored by wind speed with uniform vector lengths).

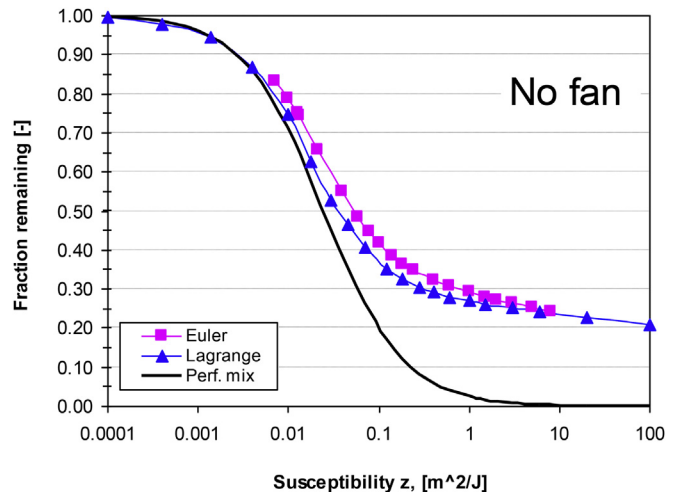


Fig. 6. Fraction remaining for the non-rotating fan case.

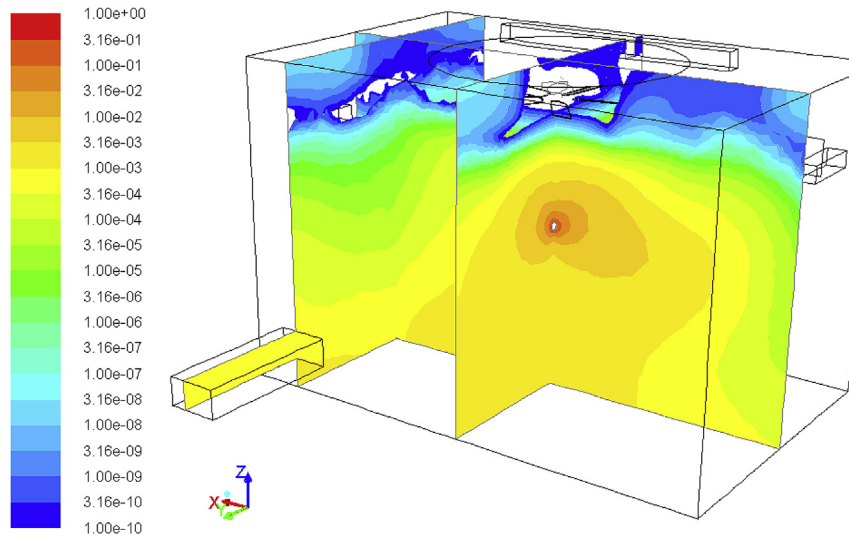


Fig. 7. Mass fraction of vital microorganisms with susceptibility $z = 8 \text{ m}^2/\text{J}$ in case 1 (non-rotating fan) [kg/kg].

measured performance with the two tested microorganisms. While system performance with *B. atrophaeus* agrees very well with predictions, measurements for *M. Parafortuitum* indicate worse performance than a perfect-mixing one. The discrepancy could be due to the large measurement uncertainty indicated by the wide confidence interval, but it is more likely due to the over-prediction of turbulence (and therefore mixing) by the realizable $k-\epsilon$ model when the problem involves multiple reference frames. This introduces discrepancy between measurements and simulations if the air is not well mixed, which will be more evident for higher susceptibilities. Therefore, it is important for the application of UR-UVGI systems to approach perfect air mixing state, which achieves equivalent exposure to UV irradiation for each microorganism.

5.3. Case 3 (medium-speed upward blowing fan)

The medium-speed upward blowing fan case also predicts a zero asymptote when the z -value approaches infinity as shown in Fig. 9, but here the agreement with measurements was excellent, especially when accounting for the tight spread of measurement data. Both measurements and simulations indicate performance close to perfect air mixing. Lagrangian predictions with two time

step selections once again demonstrate that results are independent of the time step, as long as it is kept reasonably small.

5.4. Case 4 (high-speed upward blowing fan)

The momentum created by the fan is illustrated in Fig. 10 by the velocity vectors in a vertical mid-plane. The general observation is that it was not difficult to converge the cases where the suction side of the fan was unrestricted by a solid surface. Fig. 11 shows Eulerian and Lagrangian predictions of fraction remaining vs. susceptibility. The agreement with measurements was satisfactory, however the Lagrangian method performed slightly better. Measurements with *M. parafortuitum* indicate less than perfect-mixing performance, and suggest that an increased fan speed may actually be undesirable. The explanation is that increased fan speed and mixing disperses the microorganisms throughout the room instead of efficiently transporting them upward for inactivation. Simulations predicted performance practically identical to the mid-speed case, therefore did not indicate a benefit from increased fan speed either.

A prediction of zero asymptote is a natural consequence of fan-induced upward airflow that promotes air mixing. The mixing boosts the effective scalar diffusion and increases the flux of

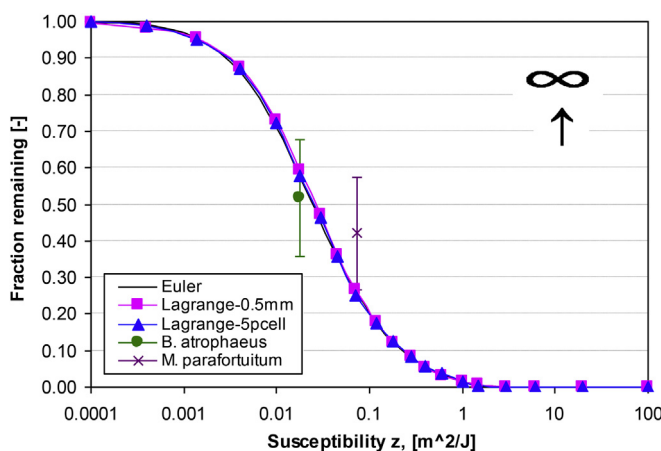


Fig. 8. Fraction remaining for low-speed upward-blown fan.

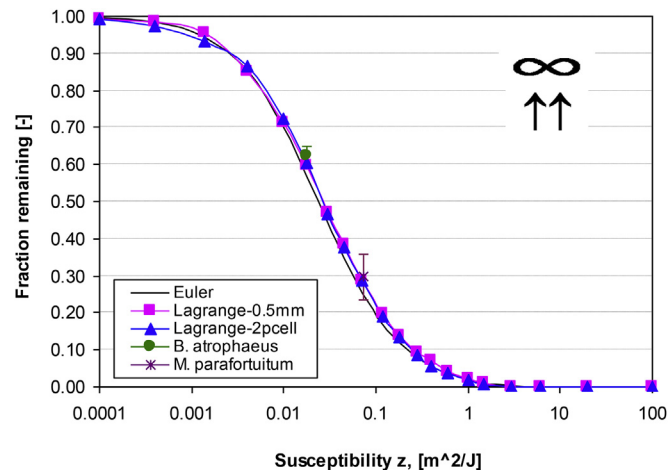


Fig. 9. Fraction remaining for medium-speed upward-blown fan.

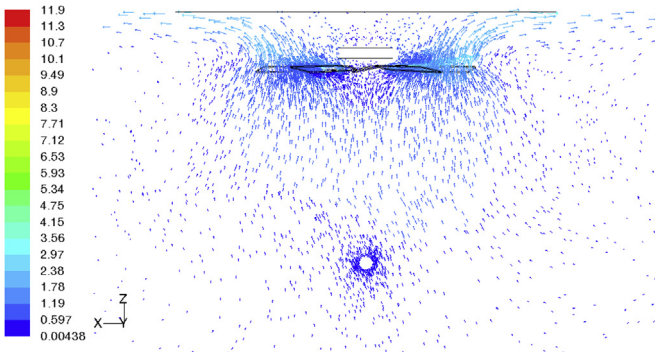


Fig. 10. Velocity vectors colored by wind speed for high-speed upward blowing fan [m/s].

microorganisms into and out of the irradiated zone, reducing the viable mass fraction at exhaust to essentially zero value, as demonstrated by the scalar distribution on Fig. 12.

5.5. Case 5 (low-speed downward blowing fan)

The downward blowing fan scenarios were significantly more difficult to converge. This is probably caused by the limited distance between the fan and ceiling, which inhibits the intake of air against the centrifugal action of the rotating blades. The Eulerian predictions were relatively unaffected by the degree of airflow convergence, but the predictions by the Lagrangian method were more sensitive. Fig. 13 shows the velocity field in a vertical room cross-section. The created momentum was not transported downward adequately, and velocities near the microorganism source were quite low ($1 \cdot 10^{-3}$ m/s). This effect renders the Eulerian approach to be a diffusion dominated one, and requires careful consideration of the microorganisms' diffusive flux at the inlet. The velocity vectors shown in Fig. 13 illustrate the circulation around the fan blade tips, resulting from the vacuum above the fan, which deflects the air upwards near the tips.

Fig. 14 presents the relationship between the fraction remaining and microorganism susceptibility. Perfect mixing performance is not achieved with this fan setup. Measurements were in agreement with this observation, and the Lagrangian method seems to be a

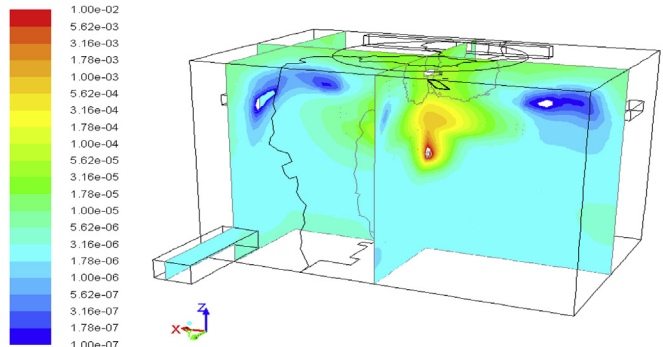


Fig. 12. Mass fraction of vital microorganisms with susceptibility $z = 8 \text{ m}^2/\text{J}$ in room with high-speed upward blowing fan [kg/kg].

better predictor once again. As explained above, the limited induction of momentum from the fan when it is close to the ceiling effectively reduces the fan-induced flow rate, resulting in reduced degrees of air mixing and limited transport of microorganisms into the irradiated zone.

5.6. Case 6 (medium-speed downward blowing fan)

Under this fan setup, both numerical methods predicted a non-zero asymptote, and thus performance inferior to the perfect mixing one, but measurements indicate this effect more clearly (Fig. 15). The likely cause for the discrepancy is again the overestimation of turbulent mixing by the turbulent model. The UVGI efficiency is more accurate than in the non-rotating fan case, but less accurate than the upward blowing fan case at the same rotational speed. Again, a possible explanation is the limited induction of fan momentum due to its close proximity to the ceiling. The measurements do not suggest a positive impact of increased fan speed compared to the low-speed case, and neither do the predictions.

5.7. Case 7 (high-speed downward blowing fan)

Predictions of the fraction of remaining microorganisms by both methods are shown in Fig. 16. The Eulerian method predicts a perfect-mixing performance, but the Lagrangian predicts an inferior one, which is a result supported by the measurements. According to these results, the downward blowing fan cases are less

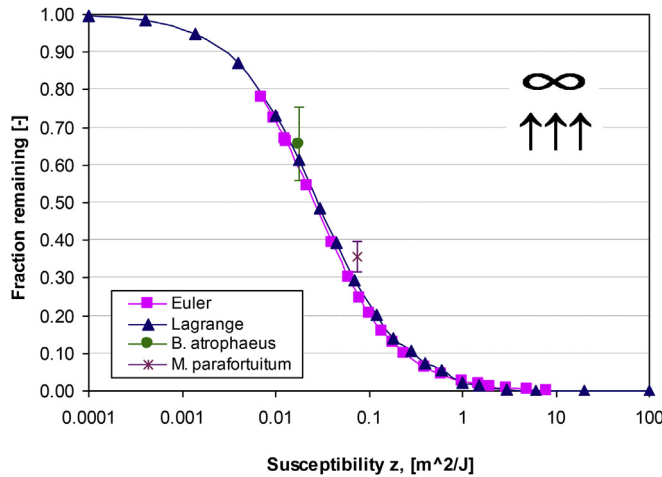


Fig. 11. Eulerian and Lagrangian predictions with measured data for high-speed upward-blowing fan case.

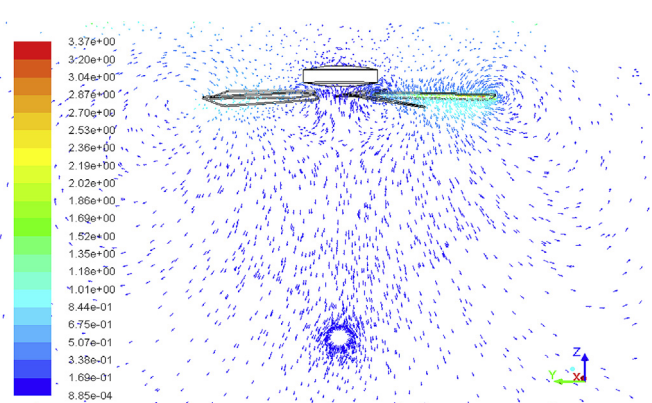


Fig. 13. Velocity vectors of uniform length, colored by wind speed in a vertical mid-plane [m/s].

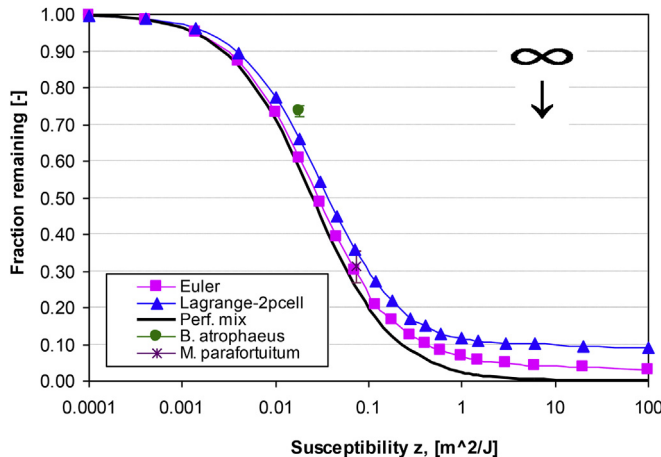


Fig. 14. Fraction remaining for low-speed downward-blowing fan case.

capable of achieving perfect-mixing performance than the upward blowing ones in an upper-room UVGI setting where microorganisms are introduced below the ceiling fan.

5.8. Result comparison and analysis

The Lagrangian computations were found to be a better predictor of performance. The inclusion of a rotating fan improved UVGI efficacy, but the benefit was more pronounced for the upward-blowing fan cases, which are compared to the perfect mixing and the non-rotating case on Fig. 17. The main advantage of the upward blowing fan is its ability to transport microorganisms generated underneath the fan into the upper zone to be irradiated before the air is well mixed. However, the increase of upward blowing fan speed only causes very slight changes in fraction remaining when the susceptibility is less than $1 \text{ m}^2/\text{J}$. Figs. 17 and 18 indicate that for small susceptibilities of less than $0.01 \text{ m}^2/\text{J}$, the system performance is virtually unaffected by the presence of a fan. However, microorganisms with minuscule susceptibility are rare, so the benefit of an upward-blowing ceiling fan is once again validated.

Fig. 18 compares all downward-blowing fan cases to the perfect-mixing and non-rotating fan cases. Inclusion of a rotating fan improves system performance, but does not achieve the nearly perfect-mixing performance of the upward-blowing fan cases. Both

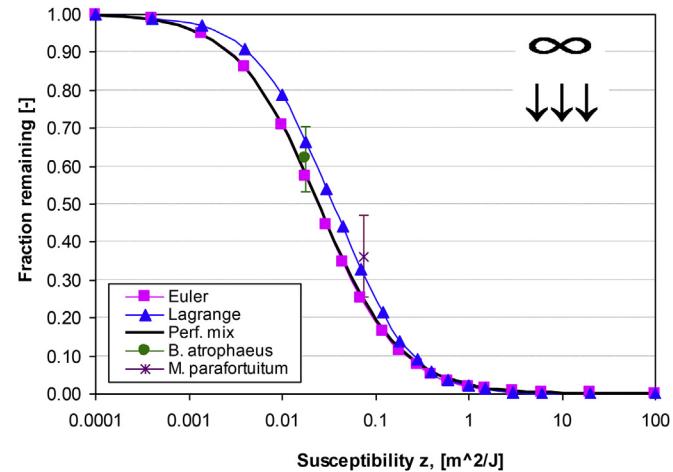


Fig. 16. Fraction remaining for high-speed downward-blowing fan case.

measurements and simulations supported the possibility that downward blow cases may not reach zero asymptote even at increased fan speed. Therefore, in hospital facilities it may be suggested that large fans blowing upward at a moderate rotational speed should be installed above the expected locations of microorganism sources. This replicates the local exhaust effect of fume-capture hoods. Overall, as shown in Figs. 17 and 18, the predictions by equation (9) are very good when using ceiling fan. According to the theory of perfect mixing [22], the use of ceiling fan shows an equivalent effect to an increase in the diffusivity of microorganisms, which increases the probability for each microorganism particle to enter the UV irradiation zone.

The curve-fit coefficients of the sigmoid function, given by equation (10), are listed in Table 3 for all simulated cases. Lower asymptotes (coefficient a) correspond to a lower fraction remaining and a higher upper-room UVGI efficacy. Non-zero asymptotes arise only in the non-rotating fan case and some downward blow cases, which cannot reach perfect-mixing performance.

6. Discussion and practical implications

The successful application of the Eulerian and Lagrangian methods for the prediction of upper-room UVGI efficiency in rooms with rotating fan is not a trivial task and presents numerous

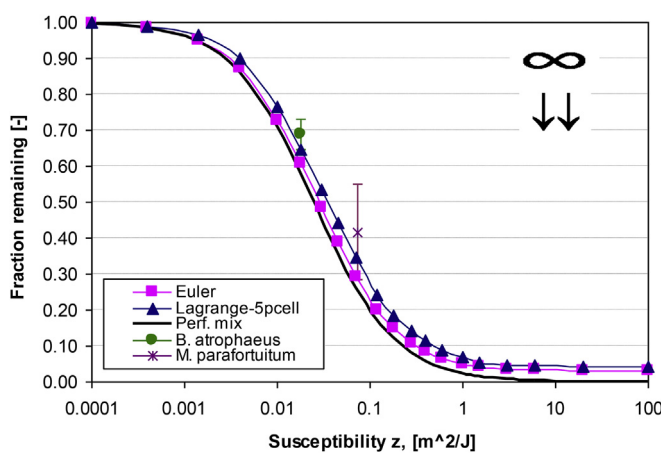


Fig. 15. Fraction remaining for medium-speed downward-blowing fan case.

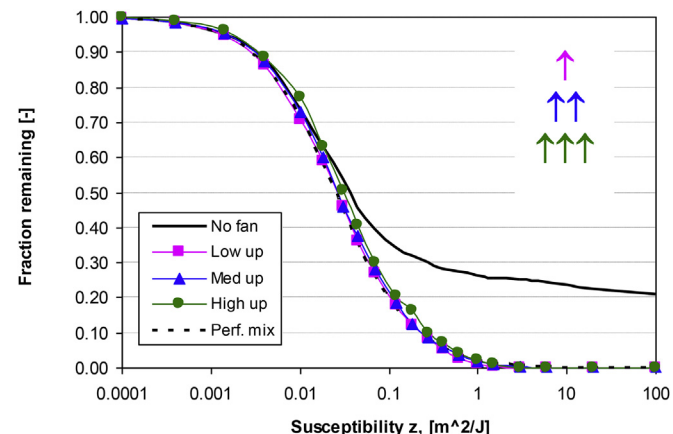


Fig. 17. Lagrangian predictions of upward blowing fan cases compared to non-rotating fan case and perfect mixing case.

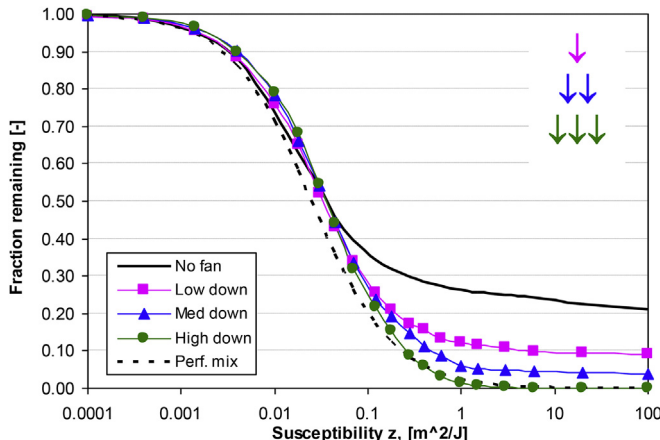


Fig. 18. Lagrangian predictions of downward blowing cases compared to non-rotating fan case and perfect mixing case.

different challenges. Both methods can perform at a satisfactory level, especially for practical design applications, but the employed software package should allow deployment of the extra numerical procedures required for this task. For example, the dose calculation and dose sampling algorithms of the Lagrangian method should be extra coded into the software package and operate concurrently with its computational algorithms to generate the correct dose values. To successfully use the Eulerian method, an option to disable the inlet scalar diffusion or an accurate method to determine the combined (convective and diffusive) scalar flux at inlets must be available. Both methods require the import of fluence rate data, which was generated by measurements in this study.

When using the Lagrangian method that calculates UV dose for each particle, the particle simulations do not need to be repeated for different microorganism species, because fraction remaining, as well as survival probability for each microorganism, is calculated with a separate stochastic procedure. However, the Eulerian method would require additional scalar simulation for each microorganism of interest. The predictions by the Lagrangian method may provide better data resolution and accuracy, but they are more sensitive to flow field convergence than the Eulerian method.

Future CFD studies can utilize the methods developed and validated in this study to further explore the impacts of room dimensions, microorganism source locations, advanced ventilation systems, novel UV lamps, fan type/size/speed/number/location, and the presence of room furniture. If a designer plans to study the impact of such parameters, it is important to understand the ability to extrapolate the simulation results to the modified setups. It

would be easiest to study the effect of changing UV lamp power. Since the microorganism inactivation depends on the product of susceptibility and fluence rate, changing the UV power (and assuming the fluence rate to change in proportion) is identical to a proportional change in the z-value under the initial setup.

Changing other design parameters will not allow for a simple extrapolation of existing results, but instead requires new simulations, either with the current computational mesh or by rebuilding the geometry and mesh. The simulation parameters that require no mesh rebuilding need only moderate effort. One such parameter is the air exchange rate, which determines the proportion between air supply and fan momentums. Another parameter is the fan rotational speed that requires changing the rotating reference frame rotation rate. In this case, it is instructive to incrementally change the rotation rate in small steps and converge the solution for each case until the target rate is reached.

There is a group of parameters that require rebuilding the case from scratch, like changing the room size or introducing furniture. Perhaps the most demanding effort would be altering the fan geometry. This concerns the size of the blades, including pitch and shape, which would require re-modeling. Fan modeling is the most demanding and time-consuming task that cannot be generally avoided since the fan's momentum dominates the flow in this type of problems. Overall, the level of effort for creating new simulations after the initial base case simulations would increase with the change of boundary conditions in the following order:

- (1) UV fixture power (lowest effort)
- (2) ACH, fan speed, source location (medium effort)
- (3) Fan type, room layout including furniture (highest effort)

7. Conclusions

The presence of a fan augments air mixing and improves upper-room UVGI system efficacy. Increasing the fan speed was only beneficial until the medium fan speed of 107 rpm, and further increase did not improve performance. Instead, in practical settings other design changes should be considered. It is optimal to install mid-speed, upward blowing fans above the microorganism source location, if it is known. UVGI efficacy predictions by Eulerian and Lagrangian methods show satisfactory agreement in simplified room configurations with adequate airflow mixing. Comparisons with experimental data identified the Lagrangian method as a better predictor, while the Eulerian tends to overestimate the UVGI efficiency due to the high degree of air mixing. The realizable $k-\epsilon$ turbulent model over-predicted the turbulent mixing when the numerical problem involves multiple reference frames. The scalar simulation creates non-realistic oscillations in the immediate vicinity of the inlet; however the effect is strictly localized and only appears when inlet diffusion is disabled. The numerical results were not sensitive to the fluence rate interpolation method, which may be due to the high degree of predicted air mixing. The impact of heat sources was insignificant compared to the dominating fan momentum in the studied cases.

Numerical predictions can be made for any indoor environment as long as the operation of the ventilation system and UV lamps are defined. For more complicated room configurations and human/flow interactions, it is believed that at least Lagrangian predictions should be correct if degree of flow turbulence is accurately predicted. The location of the microorganism source and its susceptibility to UV must be known as well. Overall, if these critical inputs for CFD simulations are unknown, it is possible to simulate microorganism disinfection under typical and critical system operating conditions. Defining these conditions remains a subject

Table 3

Curve-fit coefficients for relation between fraction remaining and z-value, equation (10) (non-zero asymptotes molded).

Case label	Blow speed	a	b	c	r^2
Case 1	N/A	0.24	1.32	69.9	0.99
Case 2	↑	0.00	1.00	38.4	0.99
Case 3	↑↑	0.00	1.00	38.3	0.99
Case 4	↑↑↑	0.00	1.00	33.5	0.99
Case 5	↓	0.10	1.10	42.2	0.99
Case 6	↓↓	0.05	1.05	32.9	0.99
Case 7	↓↓↓	0.00	1.00	26.9	0.99
Perfect mixing	N/A	0.00	1.00	40.2	1.00

The bold highlighted "a" coefficients indicate values higher than zero for the fraction of remaining, no matter how high the microorganism susceptibility or the UV field. Specifically, these three cases with residual microorganisms indicate that these airflow patterns enable survival of the microorganisms, rather than their inactivation.

for future research because the accuracy of CFD simulations for indoor environments with upper-room UVGI is mostly validated under controlled conditions, such as laboratory environments and containment facilities. Nevertheless, the greatest future potential for this technology is in the realm of preventive protection in settings where a healthy population can be exposed to an unknown or unsuspected source of microorganisms. For these kinds of studies, CFD holds great promise due to its reasonable accuracy, which has been demonstrated in this and other validation studies. An important practical outcome from these types of studies is not only an optimal solution for a particular case, but also insight that can be carried on as a CFD simulation methodology.

Air mixing conditions play a critical role in improving disinfection efficacy of UR-UVGI systems. A good mixing state for UR-UVGI application is statistically defined by the extent of how many and how soon infectious microorganisms can get inactivation. Perfect mixing is preferred as it promises an equivalent opportunity of UV irradiation exposure for each microorganism, and avoids the existence of local high levels of active microorganisms. It might not be the best strategy to minimize occupant exposure in all cases, but it is no doubt a good and safe way in most cases, especially when the locations of microorganism sources and their recipients are uncertain. The simulation results indicate that ceiling fans can achieve the performance of perfect mixing. Further, ceiling fans are able to rapidly move the infectious microorganisms away from the occupied zone and directly into UV irradiation zone for inactivation. Therefore, we believe that the proper use of ceiling fans could be beneficial to UR-UVGI applications in practice.

Acknowledgments

This work was supported by the New York State Energy Research and Development Authority (NYSERDA), under agreement 10901. The project team is grateful for Dr. Philip Brickner's indispensable experience in understanding the way to enhance patient recovery in rooms with UVGI lamps.

Nomenclature

C	microorganism mass fraction [kg/kg]
C _{UVoff}	microorganism mass fraction with UV turned OFF [kg/kg]
C _{UVon}	microorganism mass fraction with UV turned ON [kg/kg]
D	ultraviolet dose [J/m ²]
E	fluence rate [W/m ²]
f _{rm}	fraction remaining [-]
G	generation rate of microorganism [kg/s]
M	mass of air [kg]
n	number of survived microorganisms at exhaust [-]
N	total number of microorganisms at exhaust [-]
P	probability of survival [-]
z	microorganism susceptibility constant [m ² /J]
z	height [m]
\dot{m}	air mass flow rate [kg/s]
τ_n	nominal time constant [s]

References

- [1] CIE. CIE 155:2003 Ultraviolet air disinfection. 2003. Vienna, Austria.
- [2] Sliney D. Balancing the risk of eye irritation from UV-C with infection from bioaerosols. *Photochem Photobiol* 2013;89(4):770–6. <http://dx.doi.org/10.1111/php.12093>.
- [3] First MW, Nardell EA, Chaisson WT, Riley RL. Guidelines for the application of upper-room ultraviolet radiation for preventing transmission of airborne contagion—part I basic principles. *ASHRAE Trans* 1999;105(1):869–76.
- [4] First MW, Nardell EA, Chaisson WT, Riley RL. Guidelines for the application of upper-room ultraviolet radiation for preventing transmission of airborne contagion—part II. Design and design and operational guidance. *ASHRAE Trans* 1999;105(1):877–87.
- [5] NIOSH. DHHS (NIOSH) Publication No. 2009–105 Environmental control for tuberculosis: operational guidance. *ASHRAE Trans* 2009;105(1):877–87.
- [6] Zhu S, Srebric J, Rudnick SN, Nardell EA, Vincent R. Numerical approach for studying ceiling fan's influence on upper-room UVGI's disinfection efficacy. *Healthy Buildings HB2012*, July 8–12, Brisbane, Queensland. 2012.
- [7] Zhu S, Srebric J, Rudnick SN, Vincent RL, Nardell EA. Numerical investigation of upper-room UVGI disinfection efficacy in an environmental chamber with a ceiling fan. *Photochem Photobiol* 2013;89:782–91.
- [8] Zhu S, Srebric J, Rudnick SN, Vincent RL, Nardell EA. Numerical modeling of indoor environment with a ceiling fan and an upper-room ultraviolet germicidal irradiation system. *Build Environ* 2014;72:112–4.
- [9] Gilkeson CA, Noakes C. Application of CFD simulation to predicting upper-room UVGI effectiveness. *Photochem Photobiol* 2013 Jul-Aug;89(4):799–810. <http://dx.doi.org/10.1111/php.12013> [Epub 2012 Nov 28].
- [10] Noakes CJ, Sleigh PA, Fletcher LA, Beggs CB. Use of CFD modelling to optimise the design of upper-room UVGI disinfection systems for ventilated rooms. *Indoor Built Environ* 2006;15(4):347–56.
- [11] Sung M, Kato S. Method to evaluate UV dose of upper-room UVGI system using the concept of ventilation efficiency. *Build Environ* 2010;45:1626–31.
- [12] Sung M, Kato S. Estimating the germicidal effect of upper-room UVGI system on exhaled air of patients based on ventilation efficiency. *Build Environ* 2011;46:2326–32.
- [13] Kato S, Murakami S, Kobayashi H. New scales for evaluating of ventilation efficiency as affected by supply and exhaust openings based on spatial distribution of contaminant, ICCCS. In: Proc. XIth ICSS Yokohama; 1994. p. 341–8.
- [14] Kato S, Yang JH. Study on inhaled air quality in a personal air-conditioning environment using new scales of ventilation efficiency. *Build Environ* 2008;43:494–507.
- [15] Alani A, Barton IE, Seymour MJ, Wrobel LC. Application of Lagrangian particle transport model to tuberculosis (TB) bacteria UV dosing in a ventilated isolation room. *Int J Environ Health Res* 2001;11:219–28.
- [16] Xu Peng, Fisher Noah, Miller Shelly L. Using computational fluid dynamics modeling to evaluate the design of hospital ultraviolet germicidal irradiation systems for inactivating airborne mycobacteria. *Photochem Photobiol* 2013;89:792–8.
- [17] Ghia U, Konangi S, Kishore A, Gressel M, Mead K, Earnest G. Assessment of health-care worker exposure to pandemic flu in hospital rooms. *ASHRAE Trans* 2012;118(1) [CH-12-C057].
- [18] Heidarinejad M, Srebric J. Computational fluid dynamics modelling of UR-UVGI lamp effectiveness to promote disinfection of airborne microorganisms. *World Rev Sci Technol Sustain Dev* 2013;10(1/2/3):78–95.
- [19] Rudnick SN, McDevitt JJ, Hunt GM, Stawnychy MT, Vincent RL, Brickner PW. Influence of ceiling fan's speed and direction on efficacy of upper-room ultraviolet irradiation—Part 1: experimental. *Build Environ* 2014 [in press].
- [20] Kowalski WJ, Bahnfleth WP. Effective UVGI system design through improved modeling. *ASHRAE Trans* 2000;106(2):4–15 [NM-00-11-1].
- [21] Ansys Fluent v.13.0 User manual.
- [22] Roos A. On the effectiveness of ventilation [PhD thesis]. Technical University Eindhoven; 1999, ISBN 90-6814-552-5.
- [23] Rudnick SN, First MW, Sears T, Vincent RL, Brickner PW, Ngai P, et al. Spatial distribution of fluence rate from upper room ultraviolet germicidal irradiation: experimental validation of a computer-aided design tool. *HVAC&R Res* 2012;18(4):774–94.
- [24] McDevitt JJ, Rudnick SN, Radonovich LJ. Aerosol susceptibility of influenza virus to UV-C light. *Appl Environ Microbiol* March 2012;78(6):1666–9. <http://dx.doi.org/10.1128/AEM.06960-11>.